Transient and stationary transport properties of a three-subring quantum-dot structure

2008 J. Phys.: Condens. Matter 20 445216

(http://iopscience.iop.org/0953-8984/20/44/445216)

J. Phys.: Condens. Matter **20** (2008) 445216 (6pp) doi:10.1088/0953-8984/20/44/445216

Transient and stationary transport properties of a three-subring quantum-dot structure

Z T Jiang[1], J Yang[1], Y Wang[1], X F Wei[1] and Q Z Han[2]

[1] Department of Physics, Beijing Institute of Technology, Beijing 100081, People's Republic of China
[2] Multi-Phase Reaction Laboratory, Institute of Process Engineering, Chinese Academy of Sciences, PO Box 353, Beijing 100080, People's Republic of China

E-mail: jiangzhaotan@hotmail.com

Received 21 July 2008, in final form 8 September 2008
Published 10 October 2008
Online at stacks.iop.org/JPhysCM/20/445216

Abstract

A systematical investigation into the transient and stationary transport properties of a circularly coupled triple quantum-dot system including three subrings has been carried out using the modified rate equations. It is shown that both the electron-occupation probabilities and the current flowing through the triple quantum-dot structure exhibit transient oscillations in the initial stage of the quantum dynamics and eventually evolve into stationary values. Furthermore, the influences on the stationary current caused by the magnetic field and the interdot Coulomb interaction are taken into account. It is demonstrated that with a variation of the magnetic flux the current shows the $2(1 + n_1 + n_2)\pi$-period Aharonov–Bohm oscillation with $1{:}n_1{:}n_2$ being the ratio of the magnetic fluxes penetrating three subrings ϕ, $n_1\phi$, and $n_2\phi$. Moreover, although the interdot Coulomb interactions have an obvious effect upon specific oscillation behaviors, they are not able to change the oscillation period. Lastly, together with the results of the one-ring and two-subring structures, we extend the three-subring result into an N-subring case. It is verified that the Aharonov–Bohm oscillation period of the stationary current is $2(1 + n_1 + \cdots + n_{N-1})\pi$ when the ratio of the reduced magnetic flux threading into the N subrings is $1{:}n_1{:}\cdots{:}n_{N-1}$.

(Some figures in this article are in colour only in the electronic version)

1. Introduction

Quantum transport through artificial semiconductor quantum dots (QDs) has been extensively investigated in numerous publications [1–5]. Based on the Aharonov–Bohm (AB) QD interferometer, the coherence of the electron through a QD has already attracted considerable attention [6–10]. Using the AB interferometer with only one arm having an inserted QD, the electron transmission phase and the 'which-way' detector-induced dephasing were studied extensively. Then in another typical kind of AB interferometer with a QD inserted in each arm, the AB oscillation and the coherently coupled states have also been studied both experimentally [11, 12] and theoretically [13–16]. Very recently, much attention has been paid to the transport properties of a triple QD (TQD) system [17–24]. Žitko *et al* [17] determined the range of the hopping parameters where the system exhibits the two-channel Kondo effect. Jiang *et al* [19] studied theoretically the equilibrium and non-equilibrium Kondo properties of the serially coupled TQDs. Theoretically and experimentally, Korkusinski *et al* [20] analyzed the electronic structure and the charging diagram of the laterally coupled TQD. Clearly these studies indicate the three-QD or even many-QD structures are of particular interest in some aspects. However, all the above studies carried out on the TQD systems did not consider the quantum transient dynamics.

In this paper, we design a new kind of circularly coupled TQD setup (see the inset of figure 1) to investigate the transient and stationary transport properties. Obviously, three subrings exist in this TQD system, which will be called the left, middle, and right subrings for convenience. The magnetic fluxes penetrating these three subrings can be expressed as Φ_L, Φ_M, and Φ_R, respectively. It should be emphasized that this study on the versatile TQD system including three subrings can

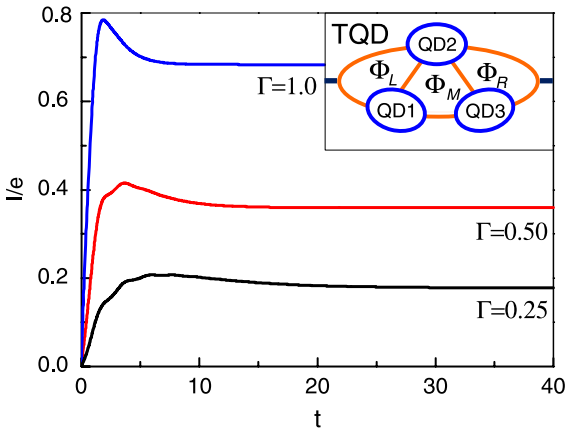

Figure 1. Time-dependent evolution of the current flowing from the left lead to the right one for different Γ in the absence of the magnetic field and the interdot Coulomb interaction. Here the interdot coupling is chosen to be $\Omega_0 = 1.0$ and the time t is in units of $1/\Omega_0$. The top-right inset shows the TQD setup studied in this paper.

also be viewed as an important starting point on the way to understanding the many-subring AB oscillation phenomena. In certain cases this TQD setup can also be simplified into a particular AB interferometer with one QD inserted in one arm and two QDs in the other one, sharply different from the usually studied AB interferometer. First of all, we derive the modified rate equations and the corresponding current of the TQD system. Then we numerically study the time-dependent evolution of the electron-occupation probabilities and the current. Also, we explore the influences of the interdot Coulomb interaction and the magnetic field. It is shown that in the initial stage the current and the probabilities show transient oscillations and eventually evolve into constants. Furthermore, it is found that the current shows AB-type periodical oscillation with the variation of the applied magnetic flux. Finally, we obtain a general relation between the current oscillation period and the magnetic field for the N-subring structure. This study should be beneficial to understanding the transport properties in this kind of structure.

The rest of this paper is organized as follows. In section 2, we present the Hamiltonian and derive the modified rate equation for the entire system. Then we analyze, in section 3, the transport properties of the TQD structure. Finally, a brief conclusion is given in section 4.

2. Model and formulae

The Hamiltonian of the entire system including three QDs and two leads can be written in the occupation number representation as $H = H_{\rm L} + H_{\rm D} + H_{\rm T}$ with[3]

$$H_{\rm L} = \sum_l \varepsilon_l a_l^\dagger a_l + \sum_r \varepsilon_r a_r^\dagger a_r, \tag{1a}$$

$$H_{\rm D} = \sum_{\alpha=1}^{3} \varepsilon_\alpha a_\alpha^\dagger a_\alpha + \sum_{\alpha<\beta}^{3} (\Omega_{\alpha\beta} a_\alpha^\dagger a_\beta + \text{h.c.}) + \sum_{\alpha<\beta}^{3} U_{\alpha\beta} n_\alpha n_\beta, \tag{1b}$$

$$H_{\rm T} = \sum_{\alpha=1}^{2} \sum_l t_{\alpha l} a_\alpha^\dagger a_l + \sum_{\beta=2}^{3} \sum_r t_{\beta r} a_\beta^\dagger a_r + \text{h.c.} \tag{1c}$$

Here $H_{\rm L}$ represents the noninteracting electron Hamiltonian of the two leads with $a_l^\dagger$ and a_l ($a_r^\dagger$ and a_r) being the corresponding creation and annihilation operators at energy level $\varepsilon_l(\varepsilon_r)$ for the electrons in the left (right) lead, respectively. The Hamiltonian of the three QDs can be described by $H_{\rm D}$, where $a_\alpha^\dagger$ (a_α) represents the creation (annihilation) operator of the electron at energy level ε_α and $n_\alpha \equiv a_\alpha^\dagger a_\alpha$ is the particle number operator. $\Omega_{\alpha\beta}$ represents the interdot coupling between QDs α and β, and $U_{\alpha\beta}$ is the corresponding interdot Coulomb interaction. $H_{\rm T}$ denotes the tunneling coupling between the QDs and the two leads, where $t_{\alpha l}$ stands for the hopping amplitude between QD-α ($\alpha = 1, 2$) and the left lead, and $t_{\beta r}$ is that between QD-β ($\beta = 2, 3$) and the right lead.

Following the procedure initially proposed by Gurvitz and Prager [25, 26], the state of the whole system can be described by the many-body wavefunction in the occupation number representation as

$$|\psi(t)\rangle = \Bigg[b_0(t) + \sum_{\alpha,l} b_{\alpha l}(t) a_\alpha^\dagger a_l + \sum_{\alpha<\beta} \sum_{l<l'} b_{\alpha\beta ll'}(t) a_\alpha^\dagger a_\beta^\dagger a_l a_{l'} + \sum_{l<l'<l''} b_{all'l''}(t) a_1^\dagger a_2^\dagger a_3^\dagger a_l a_{l'} a_{l''} + \cdots \Bigg] |0\rangle. \tag{2}$$

Here, $|0\rangle$ denotes a 'vacuum' state, in which three QDs are kept empty and all the levels in the left and right leads are initially filled with electrons up to the Fermi energy levels $\mu_{\rm L}$ and $\mu_{\rm R}$, respectively. This study is performed in the large bias ($\mu_{\rm L} \gg E_{1,2,3} \gg \mu_{\rm R}$ with $\mu_{\rm L} = -\mu_{\rm R} \to \infty$) case. $b_{\ldots}(t)$ are the time-dependent probability amplitudes of finding the system in the corresponding states. The quantum evolution of the whole system is described by the time-dependent Schrödinger equation $\mathrm{i}|\dot{\psi}(t)\rangle = H|\psi(t)\rangle$. In the eight-dimensional Fock space, consisting of states $|0\rangle$ (all QD levels are empty), $|\alpha\rangle$ (only E_α is occupied), $|\bar{\alpha}\rangle$ (only E_α is empty), and $|a\rangle$ (all QD levels are occupied), one can obtain the following Bloch-type rate equations for the diagonal elements of the density matrix $\sigma_{kk}^{(n)}(t)(k = 0, 1, 2, 3, \bar{1}, \bar{2}, \bar{3}, a)$ as

$$\dot{\sigma}_{00}^n = -(\Gamma_{\rm L1} + \Gamma_{\rm L2})\sigma_{00}^n + \Gamma_{\rm R2}\sigma_{22}^{n-1} + \Gamma_{\rm R3}\sigma_{33}^{n-1} + 2\,\mathrm{Re}(\Gamma_{\rm R}\Theta_{\rm R}\sigma_{23}^{n-1}), \tag{3a}$$

$$\dot{\sigma}_{11}^n = \Gamma_{\rm L1}\sigma_{00}^n - \Gamma_{\rm L2}^{12}\sigma_{11}^n + \Gamma_{\rm R3}\sigma_{\bar{2}\bar{2}}^{n-1} + \Gamma_{\rm R2}\sigma_{\bar{3}\bar{3}}^{n-1} + \mathrm{Re}(2\Gamma_{\rm R}\Theta_{\rm R}\sigma_{\bar{3}\bar{2}}^{n-1} - \Gamma_{\rm L}^{12}\Theta_{\rm L}\sigma_{12}^n) - 2\,\mathrm{Im}(\Omega_{21}\sigma_{12}^n + \Omega_{31}\sigma_{13}^n), \tag{3b}$$

$$\dot{\sigma}_{22}^n = \Gamma_{\rm L2}\sigma_{00}^n + \Gamma_{\rm R3}\sigma_{\bar{1}\bar{1}}^{n-1} - (\Gamma_{\rm L1}^{12} + \Gamma_{\rm R2})\sigma_{22}^n - \mathrm{Re}(\Gamma_{\rm L}^{12}\Theta_{\rm L}\sigma_{12}^n + \Gamma_{\rm R}\Theta_{\rm R}\sigma_{23}^n) - 2\,\mathrm{Im}(\Omega_{12}\sigma_{21}^n + \Omega_{32}\sigma_{23}^n), \tag{3c}$$

$$\dot{\sigma}_{33}^n = \Gamma_{\rm R2}\sigma_{\bar{1}\bar{1}}^{n-1} - (\Gamma_{\rm L1}^{13} + \Gamma_{\rm L2}^{23} + \Gamma_{\rm R3})\sigma_{33}^n - \mathrm{Re}(\Gamma_{\rm R}\Theta_{\rm R}\sigma_{23}^n) - 2\,\mathrm{Im}(\Omega_{23}\sigma_{32}^n + \Omega_{13}\sigma_{31}^n), \tag{3d}$$

[3] Usually the intradot interaction is larger than the interdot one. Here, we consider the large bias regime with $\mu_{\rm L} \gg E_i \gg \mu_{\rm R}$ and $\mu_{\rm L} \gg E_i + U_i \gg \mu_{\rm R}$ with the intradot Coulomb interaction U_i and $i = 1, 2, 3$ being the QD index. In this case, the double occupancy in each QD is allowed, weakening the influences of U_i. However, when the interdot interaction U_0 exists, we select $E_i + U_i + U_0 \gg \mu_{\rm L} \gg \mu_{\rm R}$, which will forbid the double occupancy in the corresponding QDs. Therefore, we can omit the intradot Coulomb interaction from the Hamiltonian and just keep the interdot interaction.

$$\dot{\sigma}^n_{\bar{1}\bar{1}} = -(\Gamma^a_{\rm L1} + \Gamma_{\rm R2} + \Gamma_{\rm R3})\sigma^n_{\bar{1}\bar{1}} + \Gamma^{23}_{\rm L2}\sigma^n_{33} - {\rm Re}(\Gamma^a_{\rm L}\Theta_{\rm L}\sigma^n_{\bar{2}\bar{1}}) - 2\,{\rm Im}(\Omega_{13}\sigma^n_{\bar{1}\bar{3}} + \Omega_{12}\sigma^n_{\bar{1}\bar{2}}), \quad (3e)$$

$$\dot{\sigma}^n_{\bar{2}\bar{2}} = -(\Gamma_{\rm R3} + \Gamma^a_{\rm L2})\sigma^n_{\bar{2}\bar{2}} + \Gamma^{13}_{\rm L1}\sigma^n_{\bar{3}\bar{3}} + \Gamma^{13}_{\rm R2}\sigma^{n-1}_{aa} - {\rm Re}(\Gamma_{\rm R}\Theta_{\rm R}\sigma^n_{\bar{3}\bar{2}} + \Gamma^a_{\rm L}\Theta_{\rm L}\sigma^n_{\bar{2}\bar{1}}) - 2\,{\rm Im}(\Omega_{21}\sigma^n_{\bar{2}\bar{1}} + \Omega_{23}\sigma^n_{\bar{2}\bar{3}}), \quad (3f)$$

$$\dot{\sigma}^n_{\bar{3}\bar{3}} = \Gamma^{12}_{\rm L2}\sigma^n_{11} + \Gamma^{12}_{\rm L1}\sigma^n_{\bar{2}\bar{2}} - \Gamma_{\rm R2}\sigma^n_{\bar{3}\bar{3}} + \Gamma^{12}_{\rm R3}\sigma^{n-1}_{aa} + {\rm Re}(\Gamma^{12}_{\rm L}\Theta_{\rm L}\sigma^n_{12} + \Gamma_{\rm R}\Theta_{\rm R}\sigma^n_{\bar{3}\bar{2}}) - 2\,{\rm Im}(\Omega_{31}\sigma^n_{\bar{3}\bar{1}} + \Omega_{32}\sigma^n_{\bar{3}\bar{2}}), \quad (3g)$$

$$\dot{\sigma}^n_{aa} = \Gamma^a_{\rm L1}\sigma^n_{\bar{1}\bar{1}} + \Gamma^a_{\rm L2}\sigma^n_{\bar{2}\bar{2}} - (\Gamma^{13}_{\rm R2} + \Gamma^{12}_{\rm R3})\sigma^n_{aa} + 2\,{\rm Re}(\Gamma^a_{\rm L}\Theta_{\rm L}\sigma^n_{\bar{2}\bar{1}}). \quad (3h)$$

The non-diagonal elements of the density matrix $\sigma^n_{kk'}(t)$ can be written as

$$\dot{\sigma}^n_{12} = -[\Gamma^{12}_{\rm L1} + \Gamma^{12}_{\rm L2} + \Gamma_{\rm R2}]\sigma^n_{12}/2 + \Gamma_{\rm R3}\sigma^{n-1}_{\bar{2}\bar{1}} + \Gamma_{\rm L}\Theta^*_{\rm L}\sigma^n_{00} + \Gamma_{\rm R}\Theta_{\rm R}[\sigma^{n-1}_{\bar{3}\bar{1}} - \sigma^n_{13}/2] - \Gamma^{12}_{\rm L}\Theta^*_{\rm L}[\sigma^n_{11} + \sigma^n_{22}]/2 + {\rm i}[\Omega_{12}(\sigma^n_{11} - \sigma^n_{22}) + \Omega_{32}\sigma^n_{13} - \Omega_{13}\sigma^n_{32}], \quad (4a)$$

$$\dot{\sigma}^n_{13} = -[\Gamma_{\rm R3} + \Gamma^{23}_{\rm L2} + \Gamma^{13}_{\rm L1} + \Gamma^{12}_{\rm L2}]\sigma^n_{13}/2 + \Gamma_{\rm R2}\sigma^{n-1}_{\bar{3}\bar{1}} + \Gamma_{\rm R}\Theta^*_{\rm R}[\sigma^{n-1}_{\bar{2}\bar{1}} - \sigma^n_{12}/2] + \Gamma^{12}_{\rm L}\Theta^*_{\rm L}\sigma^n_{23}/2 + {\rm i}[\Omega_{13}(\sigma^n_{11} - \sigma^n_{33}) - \Omega_{12}\sigma^n_{23} + \Omega_{23}\sigma^n_{12}], \quad (4b)$$

$$\dot{\sigma}^n_{23} = \Gamma_{\rm R}\Theta^*_{\rm R}\sigma^n_{\bar{1}\bar{1}} - [\Gamma^{13}_{\rm L1} + \Gamma^{23}_{\rm L2} + \Gamma^{12}_{\rm L1} + \Gamma_{\rm R2} + \Gamma_{\rm R3}]\sigma^n_{23}/2 - \Gamma_{\rm R}\Theta^*_{\rm R}[\sigma^n_{22} + \sigma^n_{33}]/2 - \Gamma^{12}_{\rm L}\Theta_{\rm L}\sigma^n_{13}/2 + {\rm i}[\Omega_{23}(\sigma^n_{22} - \sigma^n_{33}) + \Omega_{13}\sigma^n_{21} - \Omega_{21}\sigma^n_{13}], \quad (4c)$$

$$\dot{\sigma}^n_{\bar{1}\bar{2}} = [\Gamma^{23}_{\rm L} + \Gamma^{13}_{\rm L}]\Theta_{\rm L}\sigma^n_{33} - [2\Gamma_{\rm R3} + \Gamma^a_{\rm L1} + \Gamma^a_{\rm L2} + \Gamma_{\rm R2}]\sigma^n_{\bar{1}\bar{2}}/2 - \Gamma^a_{\rm L}\Theta_{\rm L}[\sigma^n_{\bar{1}\bar{1}} + \sigma^n_{\bar{2}\bar{2}}]/2 - \Gamma_{\rm R}\Theta^*_{\rm R}\sigma^n_{\bar{1}\bar{3}}/2 + {\rm i}[\Omega_{21}(\sigma^n_{\bar{1}\bar{1}} - \sigma^n_{\bar{2}\bar{2}}) + \Omega_{23}\sigma^n_{\bar{1}\bar{3}} - \Omega_{31}\sigma^n_{\bar{3}\bar{2}}] + {\rm i}(U_{13} - U_{23})\sigma^n_{\bar{1}\bar{2}}, \quad (4d)$$

$$\dot{\sigma}^n_{\bar{1}\bar{3}} = [\Gamma^{23}_{\rm L2} + \Gamma^{12}_{\rm L2}]\sigma^n_{31}/2 - [2\Gamma_{\rm R2} + \Gamma^a_{\rm L1} + \Gamma_{\rm R3}]\sigma^n_{\bar{1}\bar{3}}/2 + [\Gamma^{23}_{\rm L} + \Gamma^{12}_{\rm L}]\Theta_{\rm L}\sigma^n_{\bar{3}\bar{2}}/2 - \Gamma^a_{\rm L}\Theta_{\rm L}\sigma^n_{\bar{2}\bar{3}}/2 - \Gamma_{\rm R}\Theta_{\rm R}\sigma^n_{\bar{1}\bar{2}}/2 + {\rm i}[\Omega_{31}(\sigma^n_{\bar{1}\bar{1}} - \sigma^n_{\bar{3}\bar{3}}) + \Omega_{32}\sigma^n_{\bar{1}\bar{2}} - \Omega_{21}\sigma^n_{\bar{2}\bar{3}}] + {\rm i}(U_{12} - U_{23})\sigma^n_{\bar{1}\bar{3}}, \quad (4e)$$

$$\dot{\sigma}^n_{\bar{2}\bar{3}} = -[\Gamma^a_{\rm L2} + \Gamma_{\rm R2} + \Gamma_{\rm R3}]\sigma^n_{\bar{2}\bar{3}}/2 + [\Gamma^{13}_{\rm L1} + \Gamma^{12}_{\rm L1}]\sigma^n_{32}/2 - \Gamma^a_{\rm L}\Theta^*_{\rm L}\sigma^n_{\bar{1}\bar{3}}/2 + [\Gamma^{13}_{\rm L} + \Gamma^{12}_{\rm L}]\Theta^*_{\rm L}\sigma^n_{31}/2 - \Gamma_{\rm R}\Theta_{\rm R}[\sigma^n_{\bar{2}\bar{2}} + \sigma^n_{\bar{3}\bar{3}}]/2 + {\rm i}[\Omega_{32}(\sigma^n_{\bar{2}\bar{2}} - \sigma^n_{\bar{3}\bar{3}}) + \Omega_{31}\sigma^n_{\bar{2}\bar{1}} - \Omega_{12}\sigma^n_{\bar{1}\bar{3}}] + {\rm i}(U_{12} - U_{13})\sigma^n_{\bar{2}\bar{3}}. \quad (4f)$$

The other non-diagonal elements can be obtained according to the simple relation $\sigma_{kk'} = \sigma^*_{k'k}$. Here, we assume equal QD energy levels $\varepsilon_1 = \varepsilon_2 = \varepsilon_3 \equiv \varepsilon_0$, and the index n denotes the electron number found in the right lead. The energy level bandwidths are defined as $\Gamma_{\rm L1(2)} = 2\pi\rho_{\rm L}(E_1)|t_{1(2)l}|^2$ and $\Gamma_{\rm R2(3)} = 2\pi\rho_{\rm R}(E_2)|t_{2(3)r}|^2$ with $\rho_{\rm L(R)}$ denoting the density of states in the left (right) lead, which represent the rates of electron transitions from the left lead to QD-1(2) and out of QD-2(3) to the right lead, respectively. Considering the interdot Coulomb interactions (U_{12}, U_{13}, and U_{23}), we define some new parameters $\Gamma^{13}_{\rm R2}(E_1 + U_{13})$, $\Gamma^{12}_{\rm R3}(E_1 + U_{12})$, $\Gamma^{12}_{\rm L1}(E_1 + U_{12})$, $\Gamma^{12}_{\rm L2}(E_1 + U_{12})$, $\Gamma^{13}_{\rm L1}(E_1 + U_{13})$, $\Gamma^{23}_{\rm L2}(E_1 + U_{23})$, $\Gamma^a_{\rm L1}(E_1 + U_a)$, and $\Gamma^a_{\rm L2}(E_1 + U_a)$ with $U_a = U_{12} + U_{13} + U_{23}$. For simplicity, we also define $\Gamma^{12}_{\rm L} = (\Gamma^{12}_{\rm L1}\Gamma^{12}_{\rm L2})^{1/2}$, $\Gamma^{23}_{\rm L} = (\Gamma^{23}_{\rm L1}\Gamma^{23}_{\rm L2})^{1/2}$, $\Gamma^a_{\rm L} = (\Gamma^a_{\rm L1}\Gamma^a_{\rm L2})^{1/2}$, $\Gamma_{\rm R} = (\Gamma_{\rm R2}\Gamma_{\rm R3})^{1/2}$, $\Theta_{\rm L} = \exp[{\rm i}(\theta_{\rm L1} + \theta_{\rm 2L})]$, and $\Theta_{\rm R} = \exp[{\rm i}(\theta_{\rm R2} + \theta_{\rm 3R})]$. Moreover, $\Omega_{\alpha\beta} = |\Omega_{\alpha\beta}|\exp({\rm i}\theta_{\alpha\beta})$ is defined in this way to include the influences of the magnetic field, where $\theta_{\rm L1}$, $\theta_{\rm 2L}$, $\theta_{\rm R2}$, $\theta_{\rm 3R}$, θ_{12}, θ_{13}, and θ_{23} stand for the corresponding phases caused by the magnetic field. Finally, according to equation (3) we can derive the current flowing through the system as [25]

$$I(t)/e = \dot{N}_{\rm R}(t) = \sum_n n \sum_k \dot{\sigma}^n_{kk}(t) = \Gamma_{\rm R2}(\sigma_{\bar{1}\bar{1}} + \sigma_{22} + \sigma_{\bar{3}\bar{3}}) + \Gamma_{\rm R3}(\sigma_{\bar{1}\bar{1}} + \sigma_{\bar{2}\bar{2}} + \sigma_{33}) + (\Gamma^{12}_{\rm R3} + \Gamma^{13}_{\rm R2})\sigma_{aa} + 2\,{\rm Re}[\Gamma_{\rm R}\Theta_{\rm R}(\sigma_{23} + \sigma_{\bar{3}\bar{2}})]. \quad (5)$$

Clearly, the current depends on both the diagonal and non-diagonal density elements.

3. Results and discussion

In what follows, we study the transport properties of the circularly coupled TQD system numerically. For simplicity, we mainly focus on the symmetrical structure with $\Gamma_{\rm L1} = \Gamma_{\rm L2} = \Gamma_{\rm R2} = \Gamma_{\rm R3} \equiv \Gamma$ and the energy level $\varepsilon_0 = 0$. Generally, the interdot couplings are chosen to be $\Omega_{12} = \Omega_{13} = \Omega_{23} \equiv \Omega_0 = 1$ as the energy unit. We firstly consider the transient and stationary transport properties of the TQD system, and then the influences of the externally applied magnetic field and the interdot Coulomb interaction.

3.1. Transient transport

To begin with, we investigate the transient dynamics of the TQD system in the absence of the magnetic field and the interdot Coulomb interaction. Figure 1 shows the time-dependent evolution of the current I flowing through the TQD system. It is clear that the current first increases from zero and eventually evolves into a constant. This depicts how the initially unsteady TQD system approaches the stationary state. For the small $\Gamma = 0.25$, there appear some tiny oscillations in the $I \sim t$ curve at small t, which can be attributed to the electron tunneling among those three QDs. However, this kind of oscillation is completely suppressed when Γ becomes sufficiently large. It is because a larger Γ will make the system evolve into a stationary state more quickly, thus making the interdot-coupling-induced oscillation invisible. Also we can find that the value of the current at any time t increases with increasing Γ. This is reasonable since larger Γ will make it much easier for the electron to tunnel between the leads and the QDs. We believe these phenomena can be studied experimentally[4].

[4] According to the reference by Lent *et al* (see [27]) we consider a TQD system fabricated in a semiconductor with $m^* = 0.067m_0$ and the dielectric constant is $\epsilon = 10$. The interdot coupling can be taken to be $\Omega_0 \sim 0.024$ MeV and the frequency of the electron oscillating between two QDs is of the order of $\Omega_0/2\pi\hbar \sim 10^9$ Hz. In the case of $\Gamma = 1.0\Omega_0$, the current can reach the steady state in 10–100 ps. Obviously the phenomena studied here can be readily observed by using current experiment technologies.

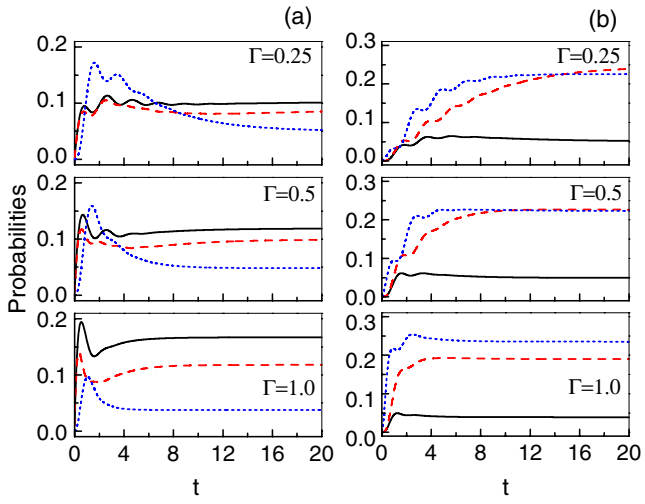

Figure 2. Time-dependent occupation probabilities of the electron with the interdot coupling $\Omega_0 = 1.0$ in the case of zero magnetic field. The occupation probabilities with only one QD occupied (σ_{11}, σ_{22}, σ_{33}) or empty ($\sigma_{\bar{1}\bar{1}}$, $\sigma_{\bar{2}\bar{2}}$, $\sigma_{\bar{3}\bar{3}}$) are shown in (a) and (b), respectively. σ_{11} and $\sigma_{\bar{1}\bar{1}}$, σ_{22} and $\sigma_{\bar{2}\bar{2}}$, σ_{33} and $\sigma_{\bar{3}\bar{3}}$ are denoted by the solid, dashed, and dotted curves, respectively. The time t is in units of $1/\Omega_0$.

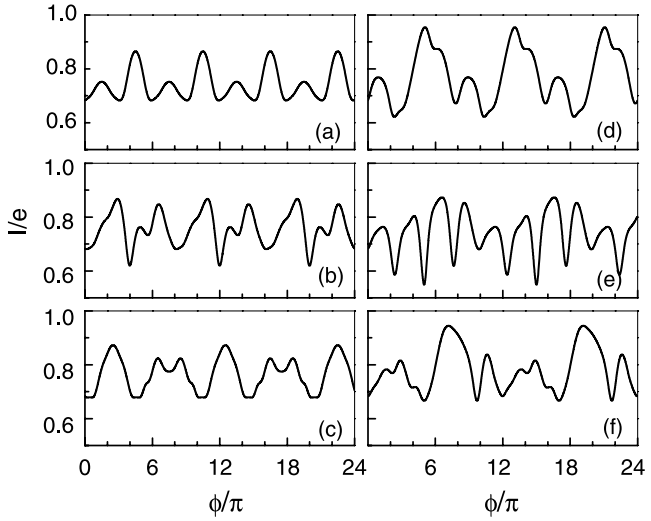

Figure 3. Variation of the stationary current I as a function of the reduced magnetic flux ϕ with $U = 0$, $\Gamma = 1$, and $\Omega_0 = 1$ for different reduced magnetic flux ratios (a) 1:1:1, (b) 1:1:2, (c) 1:1:3, (d) 1:2:1, (e) 1:2:2, and (f) 1:2:3, respectively.

In order to get an intuitive understanding on what induces the current variation, it is very necessary to conduct an in-depth investigation into the density matrices. So, we show in figure 2 the corresponding electron-occupation probabilities as a function of time t for different Γ. For the weak coupling $\Gamma = 0.25$, the curves of $\sigma_{\alpha\alpha}$ and $\sigma_{\bar{\alpha}\bar{\alpha}}$ ($\alpha = 1, 2, 3$) show transient oscillations at small t, which demonstrates that the electrons are able to tunnel among those three QDs. After a long enough time all of the probabilities become independent of time, indicating that the TQD system has evolved into a steady state. It is this kind of oscillating probability that leads to the current variations. Furthermore, we can see as Γ increases, the probabilities will evolve into steady states more quickly. Microscopically this demonstrates that the system will evolve into a stationary state after a sufficiently long time.

Then we examine the details of the time-dependent probabilities. From the curves of $\Gamma = 0.25$ in the figure 2(a), we can find that the σ_{11} curve overlaps with the σ_{22} one at small $t \to 0$. As the time goes on, however, σ_{22} is inclined to become smaller than σ_{11}. This can be understood according to an intuitive tunneling picture. Firstly, the electrons in the left lead can tunnel simultaneously into both QD1 and QD2 at the same speed. As a result σ_{11} and σ_{22} are kept equal in the initial time. Then both the electrons in QD1 and those in QD2 can flow into the right lead by passing through the QD3 channel. However, the electrons in QD2 have one more channel to use to enter the right lead. Therefore, the probability σ_{22} will decrease more quickly than σ_{11}, causing $\sigma_{22} < \sigma_{11}$ even in the stationary state. On the other hand, it is clear that σ_{33} is smaller than σ_{11} and σ_{22} in the initial stage. This is because the electrons incident from the left lead will first enter QD1 and QD2, and then enter QD3. Moreover, the specific values of the probabilities in the stationary state will change a lot for different Γ. Actually, the variations of these stationary values corresponding to different Γ are determined only by the transient process in the unstable stage since in the stationary state the number of the input electrons from the left lead is equal to that out of the central three QDs.

3.2. Magnetic field effect

In the following we will focus on the influences of the magnetic field on the stationary transport through the TQD in two cases: $U = 0$ and ∞. The reduced magnetic fluxes penetrating three subrings are denoted by ϕ_L, ϕ_M, and ϕ_R, respectively[5]. Their effects can be taken into account by introducing some phases $\theta_{12}, \theta_{23}, \theta_{L1}, \theta_{2L}, \theta_{13}, \theta_{R2}$, and θ_{3R}. For convenience, we assume $\theta_{12} = \theta_{23} = 0$, $\theta_{L1} + \theta_{2L} = \phi_L$, $\theta_{13} = \phi_M$, $\theta_{R2} + \theta_{3R} = \phi_R$ with the total reduced magnetic flux $\phi = \phi_L + \phi_M + \phi_R$.

Firstly we examine how the distribution (the flux ratio $\gamma \equiv \phi_L{:}\phi_M{:}\phi_R$) of the magnetic field in the three subrings affects the stationary transport, especially the period of the current oscillation. In figure 3 we plot the variation of the stationary current as a function of the total reduced magnetic flux ϕ for the different reduced magnetic flux ratios γ. We can see from figure 3(a) that the stationary current exhibits a periodic oscillation with a period of 6π when $\gamma = 1{:}1{:}1$. Obviously this is sharply different from the usual single-ring AB oscillation with a period of 2π [6]. Furthermore, one can find that the oscillation period varies with γ by comparing the curves in figures 3(a)–(f). The currents oscillate with the periods of 8π, 10π, 8π, 10π, and 12π in response to different reduced magnetic flux ratios $\gamma = 1{:}1{:}2$, $1{:}1{:}3$, $1{:}2{:}1$, $1{:}2{:}2$, and $1{:}2{:}3$, respectively. Thus, we can conclude that the stationary current shows the oscillation with a period of $2\pi\xi$ when the ratio γ of the reduced magnetic fluxes in the three subrings is equal to $1{:}n_1{:}n_2$ (here we introduce $\xi = 1 + n_1 + n_2$). For a general case

[5] The reduced magnetic fluxes $\phi_{L,M,R} = 2\pi\Phi_{L,M,R}/\Phi_0$ with $\Phi_0 = h/e$ being the magnetic flux quanta.

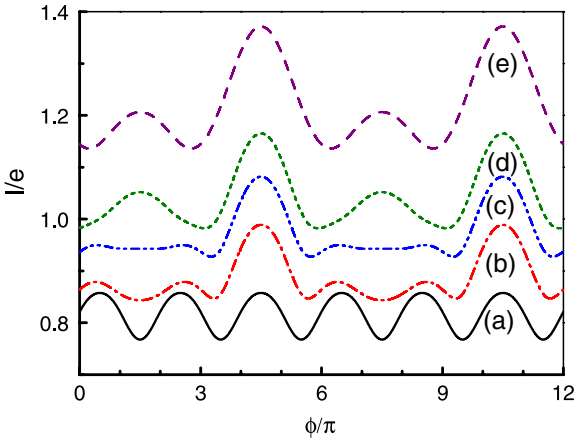

Figure 4. Variation of the stationary current as a function of the reduced magnetic flux for different interdot couplings $\Omega_{12} = \Omega_{23} = \Omega$. Here, the energy level bandwidth is $\Gamma = 1.0$, the interdot coupling Ω_{13} is selected to be 1.0 and the reduced magnetic flux ratio is $\gamma = 1{:}1{:}1$. For clarity, the curves of (a) $\Omega = 0.0$, (b) $\Omega = 0.5$, (c) $\Omega = 0.65$, (d) $\Omega = 1.0$, (e) $\Omega = 2.0$ are shifted upward by 0.0, 0.1, 0.2, 0.3, 0.4, respectively.

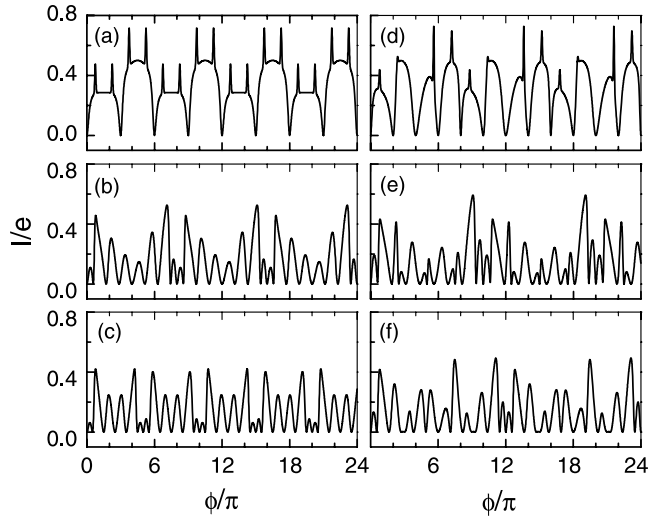

Figure 5. Variation of the stationary current as a function of the reduced magnetic flux ϕ in the case of $U = \infty$, $\Gamma = 1.0$, and $\Omega_0 = 1.0$ for different reduced magnetic flux ratios (a) 1:1:1, (b) 1:1:2, (c) 1:1:3, (d) 1:2:1, (e) 1:2:2, and (f) 1:2:3, respectively.

the ratio of the magnetic fluxes may be $\gamma = 1{:}l_1{:}l_2$ with l_1 and l_2 being noninteger. It seems difficult to infer the oscillation period based on the above results of $\gamma = 1{:}n_1{:}n_2$. However, γ just determines the partition of the magnetic fluxes penetrating three subrings in nature. Therefore, we can convert an arbitrary ratio $\gamma = 1{:}l_1{:}l_2$ into a new form of $n_1{:}n_2{:}n_3$ with integer n_1, n_2, and n_3. Thus the oscillation period can be calculated in the usual way: $2\pi(n_1 + n_2 + n_3)$. For example, $\gamma = 1{:}0.2{:}1.2$ can be transformed into 5:1:6, which clearly depicts the partition of the magnetic fluxes $\Phi_L{:}\Phi_M{:}\Phi_R = 5{:}1{:}6$. Therefore, the oscillation period should be $2\pi(5 + 1 + 6) = 24\pi$. Thus we have generalized our study into the general case with arbitrary magnetic flux ratio γ.

As is well known, the current flowing through the single-ring setup oscillates with a period of 2π. Obviously, the oscillation behaviors of the current through the three-subring system studied here are completely different. Therefore, we utilize our TQD system to explore the transition process from the 2π-period current oscillation of the single AB ring to the 6π-period oscillation of the triple AB ring. So we show in figure 4 the currents for the different interdot couplings $\Omega_{12} = \Omega_{23} = \Omega$ at long enough time $t = 100$ with $\gamma = 1{:}1{:}1$. Clearly, in the case of $\Omega = 0$ the three-subring system becomes a single-ring setup. As expected, the stationary current exhibits a 2π-period oscillation. When the interdot coupling Ω turns on, three subrings are formed immediately and the feature of the corresponding current changes substantially. The oscillation period changes from 2π to 6π, which results from the geometry variation from the single-ring to the three-subring system. When Ω increases further, the trough at about $\phi = 1.5\pi$ will be inclined to vanish and eventually evolves into a peak. In the meantime, the size of this peak submerges the two peaks localized at $\phi = 0.5\pi$ and 2.5π. However, the peak at $\phi = 4.5\pi$ continuously increases with the increasing of Ω to form the largest peak, as shown in the curve of $\Omega = 2.0$. These verify that the specific oscillation behavior is closely dependent on the interdot couplings and the 2π-to-6π transition is determined only by the geometric structure.

Finally, we discuss the influences of the interdot Coulomb interaction U on the period of the current oscillation. Figure 5 shows the stationary current for the different flux ratios γ when $U = \infty$. In comparison with the $U = 0$ case shown in figure 3, extremely obvious changes have happened in the oscillation patterns. However, the oscillation periods are always kept invariant for any γ. That is to say, even in the case of $U = \infty$ the current still oscillates with a period of $2\pi(1+n_1+n_2)$ when the reduced magnetic flux ratio is $\gamma = 1{:}n_1{:}n_2$. This verifies that the interdot Coulomb interaction does change the specific oscillation of the current, but does not affect the oscillation period induced by the threaded magnetic field.

3.3. Analytic discussion and extension

To analytically explain the period of the current oscillation, we can list the seven main channels (1) L $\rightarrow$ QD2 $\rightarrow$ R, (2) L $\rightarrow$ QD2 $\rightarrow$ QD3 $\rightarrow$ R, (3) L $\rightarrow$ QD1 $\rightarrow$ QD2 $\rightarrow$ R, (4) L $\rightarrow$ QD1 $\rightarrow$ QD3 $\rightarrow$ R, (5) L $\rightarrow$ QD1 $\rightarrow$ QD2 $\rightarrow$ QD3 $\rightarrow$ R, (6) L $\rightarrow$ QD1 $\rightarrow$ QD3 $\rightarrow$ QD2 $\rightarrow$ R, and (7) L $\rightarrow$ QD2 $\rightarrow$ QD1 $\rightarrow$ QD3 $\rightarrow$ R for the electron to transport from the left lead to the right one. The electron flowing through these channels can be described as $\Lambda_\alpha = A_\alpha \exp(\mathrm{i}P_\alpha)$ with $\alpha = 1, 2, \cdots, 7$, respectively. To be specific, we have $P_1 = \theta_{2L} + \theta_{R2}$, $P_2 = \theta_{2L} + \theta_{32} + \theta_{R3}$, $P_3 = \theta_{1L}+\theta_{21}+\theta_{R2}$, $P_4 = \theta_{1L}+\theta_{31}+\theta_{R3}$, $P_5 = \theta_{1L}+\theta_{21}+\theta_{32}+\theta_{R3}$, $P_6 = \theta_{1L} + \theta_{31} + \theta_{23} + \theta_{R2}$, and $P_7 = \theta_{2L} + \theta_{12} + \theta_{31} + \theta_{R3}$. So, the total wavefunction can be written as

$$\Lambda_T = \sum_{\alpha=1}^{7} \Lambda_\alpha. \tag{6}$$

Then we can obtain the probability of finding the electron in the right lead

$$|\Lambda|^2 = \sum_{\alpha=1}^{7} |\Lambda_\alpha|^2 + 2 \sum_{\alpha,\beta=1}^{7} |\Lambda_\alpha||\Lambda_\beta| \cos P_{\alpha\beta}, \qquad (7)$$

where the first term in the right-hand side of equation (7) denotes the direct transport through the seven channels, and the second one is the coherent component among those channels. $P_{\alpha\beta} = P_\alpha - P_\beta$ represents the phase difference between the αth channel and the βth one. When the reduced magnetic fluxes threading into the three subrings are selected to be $\phi_L = \phi/\xi$, $\phi_M = n_1\phi/\xi$, and $\phi_R = n_2\phi/\xi$, the phase differences can be explicitly expressed as $P_{14} = P_{26} = P_{37} = \phi$, $P_{13} = P_{25} = P_{47} = \phi/\xi$, $P_{27} = P_{36} = P_{45} = n_1\phi/\xi$, $P_{12} = P_{35} = P_{46} = n_2\phi/\xi$, $P_{16} = P_{24} = P_{57} = (1+n_1)\phi/\xi$, $P_{15} = P_{23} = P_{67} = (1+n_2)\phi/\xi$, and $P_{17} = P_{34} = P_{56} = (n_1+n_2)\phi/\xi$. Therefore, the corresponding oscillation periods of the functions $\cos P_{\alpha\beta}$ in equation (7) certainly equal 2π, $2\xi\pi$, $2\xi\pi/n_1$, $2\xi\pi/n_2$, $2\xi\pi/(1+n_1)$, $2\xi\pi/(1+n_2)$, and $2\xi\pi/(n_1+n_2)$, respectively. Thus one can readily find that the total period of $|\Lambda|^2$ should be $2\xi\pi = 2\pi(1+n_1+n_2)$. Analytically, we verified that the current flowing through a three-subring setup should oscillate with a period of $2\pi(1+n_1+n_2)$, which is independent of the number of QDs in the setup, the interdot couplings, the interdot Coulomb interaction, and so on.

Together with the 2π-period AB oscillation in the one-ring setup, as well as the $2\pi(1+n_1)$-period AB oscillation of the two-subring setup, we can extend the result $2\pi(1+n_1+n_2)$ of the three-subring setup into an N-subring system. The period of the magnetic-field-induced AB current oscillation should be $2\pi(1+n_1+n_2+\cdots+n_{N-1})$ when the ratio of the magnetic flux threading into the N subrings is $1{:}n_1{:}n_2{:}\cdots{:}n_{N-1}$. We believe this result should be universal for the mesoscopic setup, which is helpful in understanding the coherent transport in such many-subring systems.

4. Conclusion

In conclusion, we have firstly derived the modified rate equations of the TQD system including three subrings. It is shown that the current and the probabilities of the electrons occupying the QDs exhibit transient oscillations in the initial stage and become constants eventually, indicating the system has evolved into a stationary state. Moreover, we find that the current shows $2\pi(1+n_1+n_2)$ period oscillation with the increase of the magnetic field, when the reduced magnetic fluxes threaded through the three subrings are ϕ, $n_1\phi$, and $n_2\phi$. It is also verified that the oscillation period is not influenced by the interdot Coulomb interaction. Based on an analytical explanation, we extend our results to the N-subring system, which can be viewed as a useful reference in understanding N-subring transport properties.

Acknowledgments

This work is financially supported by the NSFC under grant Nos 10547105 and 10604005, and the Excellent Young Scholars Research Fund of Beijing Institute of Technology (No. 2006Y0713).

References

[1] Goldhaber-Gordon D, Göres J, Kastner M A, Shtrikman H, Mahalu D and Meirav U 1998 *Phys. Rev. Lett.* **81** 5225
[2] Cronenwett S M, Oosterkamp T H and Kouwenhoven L P 1998 *Science* **281** 540
[3] You J Q and Zheng H Z 1999 *Phys. Rev.* B **60** 13314
[4] Sun Q F, Wang J and Lin T-H 1999 *Phys. Rev.* B **60** R13981
[5] Li S S, Xia J B, Yuan Z L, Xu Z Y, Ge W K, Wang X R, Wang Y, Wang J and Chang L L 1996 *Phys. Rev.* B **54** 11575
[6] Yacoby A, Heiblum M, Mahalu D and Shtrikman H 1995 *Phys. Rev. Lett.* **74** 4047
Yacoby A, Schuster R and Heiblum M 1996 *Phys. Rev.* B **53** 9583
[7] Schuster R, Buks E, Heiblum M, Mahalu D, Umansky V and Shtrikman H 1997 *Nature* **385** 417
[8] Buks E, Schuster R, Heiblum M, Mahalu D and Umansky V 1998 *Nature* **391** 871
[9] Sun Q F, Wang J and Guo H 2005 *Phys. Rev.* B **71** 165310
[10] Baltin R and Gefen Y 1999 *Phys. Rev. Lett.* **83** 5094
[11] Holleitner A W, Decker C R, Qin H, Eberl K and Blick R H 2001 *Phys. Rev. Lett.* **87** 256802
[12] König J and Gefen Y 2002 *Phys. Rev.* B **65** 045316
[13] Ladrón de Guevara M L, Claro F and Orellana P A 2003 *Phys. Rev.* B **67** 195335
[14] Jiang Z T, You J Q, Bian S B and Zheng H Z 2002 *Phys. Rev.* B **66** 205306
[15] Kubala B and König J 2002 *Phys. Rev.* B **65** 245301
[16] Ding G H, Kim C K and Nahm K 2005 *Phys. Rev.* B **71** 205313
[17] Žitko R and Bonča J 2007 *Phys. Rev. Lett.* **98** 047203
Žitko R, Bonča J, Ramšak A and Rejec T 2006 *Phys. Rev.* B **73** 153307
[18] Ladrón de Guevara M L and Orellana P A 2006 *Phys. Rev.* B **73** 205303
[19] Jiang Z T, Sun Q F and Wang Y P 2005 *Phys. Rev.* B **72** 045332
[20] Korkusinski M, Gimenez I P, Hawrylak P, Gaudreau L, Studenikin S A and Sachrajda A S 2007 *Phys. Rev.* B **75** 115301
[21] Kuzmenko T, Kikoin K and Avishai Y 2006 *Phys. Rev. Lett.* **96** 046601
[22] Hur K L, Recher P, Dupont É and Loss D 2006 *Phys. Rev. Lett.* **96** 106803
[23] Gaudreau L, Studenikin A, Sachrajda A S, Zawadzki P, Kam A, Lapointe J, Korkusinski M and Hawrylak P 2006 *Phys. Rev. Lett.* **97** 036807
[24] Li Y X 2007 *J. Phys.: Condens. Matter* **19** 496219
[25] Gurvitz S A and Prager Ya S 1996 *Phys. Rev.* B **53** 15932
[26] Gurvitz S A 1998 *Phys. Rev.* B **57** 6602
Gurvitz S A 2000 *Phys. Rev. Lett.* **85** 812
[27] Lent C S 1993 *Appl. Phys. Lett.* **62** 714